processes

MDPI

*Article*

# The Thermodynamic Characterizations of Hydrogen Production from Catalyst-Enhanced Steam Reforming of Bio-Oil over Granulated Blast Furnace Slag as Heat Carrier

**Zhijun Ding [1], Yang Liu [2], Xin Yao [1,*], Yuekai Xue [1,*], Chenxiao Li [1,*], Zhihui Li [1], Shuhuan Wang [1] and Jianwei Wu [3]**

[1] College of Metallurgy and Energy, North China University of Science and Technology, Tangshan 063210, China; sgdingzhijun@hbisco.com (Z.D.); lzh@ncst.edu.cn (Z.L.); wshh88@ncst.edu.cn (S.W.)
[2] Health Center, North China University of Science and Technology, Tangshan 063210, China; liuyangineur@outlook.com
[3] School of Metallurgy, Northeastern University, Liaoning 110819, China; wujianweiup@163.com
* Correspondence: yaoxin_0129@163.com (X.Y.); xueyuekai965@163.com (Y.X.); lichenxiao34@163.com (C.L.)

**Abstract:** To promote the efficiency of waste heat recovery from granulated blast furnace (BF) slag, a novel method of catalyst-enhanced steam reforming of bio-oil to recover heat from slag is proposed. CaO is utilized as a superior catalyst for the process of catalyst-enhanced steam reforming. The thermodynamic production of the catalyst-enhanced steam reforming of bio-oil in granulated BF slag is obtained using HSC 6.0 software. The optimal conditions are mainly assessed according to the hydrogen yield, hydrogen concentration and carbon production. Through the thermodynamic production and industrial application, the temperature of 608 °C, S/C of eight and pressure of 1 bar are found as the optimal conditions. At the optimal conditions, the hydrogen yield, hydrogen concentration and carbon production are 95.25%, 76.89% and 0.28 mol/kg, respectively. Taking the temperature of 625 °C, S/C of eight and pressure of 1 bar as an example, the catalyst could improve the hydrogen yield and hydrogen concentration from 93.99% and 70.31% to 95.15% and 76.49%, respectively. It is implied that utilizing the catalyst could promote the hydrogen yield and hydrogen concentration of steam reforming of bio-oil to recover waste heat from granulated BF slag. The mechanism of catalyst-enhanced steam reforming of bio-oil to recover waste heat from granulated BF slag is obtained to guide the subsequent industry application.

**Keywords:** catalyst-enhanced steam reforming; granulated BF slag; heat recovery; thermodynamic analysis



**Citation:** Ding, Z.; Liu, Y.; Yao, X.; Xue, Y.; Li, C.; Li, Z.; Wang, S.; Wu, J. The Thermodynamic Characterizations of Hydrogen Production from Catalyst-Enhanced Steam Reforming of Bio-Oil over Granulated Blast Furnace Slag as Heat Carrier. *Processes* **2023**, *11*, 2341. https://doi.org/10.3390/pr11082341

Academic Editor: Adam Smoliński

Received: 30 June 2023
Revised: 29 July 2023
Accepted: 2 August 2023
Published: 3 August 2023



## 1. Introduction

The emissions of carbon dioxide can lead to global warming, damaging the ecological balance seriously [1,2]. In order to achieve sustainable development, China, which contributes the highest annul carbon emissions in the world, proposed the "dual carbon goals" in 2022 and pledges to peak its carbon dioxide before 2030 and achieve carbon neutrality before 2060. Driven by the carbon peaking action plan, the iron and steel industries are accelerating their green transformation and development to achieve energy conservation and emission reduction [3–5].

According to the statistics, pig iron production is 868.6 Mt in China in 2021 [6], which is the biggest in the world. Additionally, 90% of pig iron in China is obtained via blast furnace (BF), and about 260.2 Mt of BF slag with a temperature of 1550 °C is obtained [7]. The BF slag, which has shown low thermal conductivity and easy crystallization behavior, is disposed via the water quenching method in the industry application. The water quenching slag is used as the raw material for cement production. But huge amounts of high-quality energy are wasted during the water quenching process. The appropriate treatment of BF

slag is regarded as a promising method to achieve green development of the iron and steel industry.

BF slag is mainly applied as a raw material for cement production. Granulated BF slag produced using a rotary cup atomizer (RCA) with high grassy content is also used as the raw material for cement product [8–10]. But the temperature of granulated BF slag obtained via RCA is higher than 1000 °C [11,12]. The granulated BF slag carries enormous high-quality energy. Searching for a reasonable method to recover waste heat from granulated BF slag is regarded as an outstanding method to reduce energy consumption in the iron and steel industry. Physical methods and chemical methods were proposed to recover waste heat from granulated BF slag [13]. Li investigated the advantages of chemical methods and physical methods to recover waste heat from slag using an enthalpy exergy compass, proving that the energy efficiency and exergy efficiency using the chemical method were higher than those when using the physical method [14]. Some chemical methods attempt to recover waste heat from granulated BF slag have been proceeded in recent years. Purwanto [15] first proposed using biogas to recover waste heat from granulated BF slag. The results implied that granulated BF slag could replace the energy required for hydrogen production and be beneficial for the process of biogas reaction. Subsequently, Zhao [16] investigated the gasification of municipal solid waste to recover waste heat from granulated BF slag. The results implied that granulated BF slag could catalyze the process of municipal solid waste gasification, which could be regarded as a superior heat carrier. Additionally, applying coal gasification [17,18], biomass gasification [19–21], biomass pyrolysis [22,23], sludge gasification [24,25] and sludge pyrolysis [4,5] to recover waste heat from granulated BF were proposed. The results implied that granulated BF slag containing metal ions such as $Ca^{2+}$ and $Fe^{3+}$ could weaken the C-C bond and C-H bond, catalyzing the process of these reactions. In addition, the kinetic parameters, such as the activation energies and pre-exponential factors of coal gasification [18], biomass gasification [7] in granulated BF slag was achieved via thermogravimetric analysis. The results implied that slag could decrease the activation energy of these reactions, proving that slag could catalyze these reactions according to thermodynamic analysis.

In the 21st century, hydrogen is regarded as a green energy to replace fossil fuels [26,27]. Bio-oil reforming is one of the effective methods to obtain hydrogen [28,29], but the process of bio-oil reforming requires energy. Based on the advantages of chemical reactions to recover waste heat from granulated BF slag, Yao proposed bio-oil reforming over granulated BF slag as a heat carrier [30–32]. The results implied that granulated BF slag had a positive effect on the bio-oil reforming process, but the positive effect was insignificant, particularly at low temperatures. Additionally, Sun investigated the equilibrium productions of biomass gasification [33] and biomass pyrolysis [3] in the slag, also proving that slag had a little effect on the hydrogen yield and equilibrium production.

Utilization of biogas [15], municipal solid waste gasification [16], coal gasification [17,18], biomass gasification [19–21], biomass pyrolysis [22,23], sludge gasification [24,25], sludge pyrolysis [4,5] and bio-oil reforming [30–32] to recover waste heat from granulated BF have been proposed. These studies did not involve catalyst-enhanced chemical reactions to recover waste heat from granulated BF slag. Promoting chemical reaction rates in granulated BF slag is regarded as a promising research direction for recovering waste heat from slag. However, the study is scarce. In this paper, the catalyst-enhanced steam reforming of bio-oil to recover waste heat from granulated BF slag is proposed. Meanwhile, CaO could catalyze the steam reforming of the bio-oil process and be obtained easily during the industry production [34–36]. Thus, CaO is utilized as the catalyst for bio-oil reforming to recover waste heat from granulated BF slag. This paper investigates the equilibrium productions of the catalyst-enhanced steam reforming of bio-oil in granulated BF slag via thermodynamic calculation. The optimal conditions are obtained. The mechanism of catalyst-enhanced steam reforming of bio-oil over granulated BF is illustrated. These results will prove the advantages of the method and promote the basic thermodynamic data in the industry application.

## 2. Methodology

### *2.1. Raw Materials*

Bio-oil is a macromolecular carbon oxyhydroxide, whose components are complex [37,38]. To facilitate the characterization of steam reforming of bio-oil, the bio-oil model compound is applied to replace bio-oil [39,40]. The principal components of bio-oil are alcohols, acids, ketones and phenols [41]. Therefore, the model compound of bio-oil is applied to simulate the composition of bio-oil. It consists of an equal-mass-ratio mixture of ethanol, acetic acid, acetone and phenol [30,32]. The components of the model compound of bio-oil is shown in Table 1.

**Table 1.** The components in the model compound of bio-oil [30,32].

| Component | Ethanol | Acetic Acid | Acetone | Phenol |
|---|---|---|---|---|
| Mass fraction | 25% | 25% | 25% | 25% |

Granulated BF slag obtained via RCA is regarded as a superior raw material to produce cement. The detailed preparation method and properties of granulated BF slag were obtained in previous studies [23,31,42,43]. The mass ratio of the model compound of bio-oil and the granulated BF slag is 1:1.

### *2.2. Catalyst-Enhanced Steam Reforming Reactions*

The process of catalyst-enhanced steam reforming of bio-oil in granulated BF slag contains coupled reactions, such as the thermal cracking reaction, steam reforming reactions, methanation reactions, water gas reaction, water gas shift reaction, Bell reaction and reactions of mineral oxide with the generated gases. The main equations of catalyst-enhanced steam reforming of bio-oil in granulated BF slag are shown in Table 2.

**Table 2.** The main equations of catalyst-enhanced steam reforming of bio-oil in granulated BF slag [30].

| Name | Equations | No. |
|---|---|---|
| Thermal cracking reaction | $\text{Bio-oil} \rightarrow o\text{H}_2 + p\text{CO} + q\text{CO}_2 + r\text{CH}_4 + s\text{C},\ \Delta\text{H}^{\theta}_{800\ ^{\circ}\text{C}} > 0$ | (1) |
| | $\text{C}_x\text{H}_y\text{O}_z + (2x - z)\text{H}_2\text{O} \rightarrow x\,\text{CO}_2 + (2x + y/2 - z)\text{H}_2,\ \Delta\text{H}^{\theta}_{800\ ^{\circ}\text{C}} > 0$ | (2) |
| Steam reforming reactions | $\text{C}_2\text{H}_6\text{O} + 3\text{H}_2\text{O} \rightarrow 2\,\text{CO}_2 + 6\text{H}_2,\ \Delta\text{H}^{\theta}_{800\ ^{\circ}\text{C}} = 210.26\ \text{kJ/mol}$ | (3) |
| | $\text{C}_2\text{H}_4\text{O}_2 + 2\text{H}_2\text{O} \rightarrow 2\,\text{CO}_2 + 4\text{H}_2,\ \Delta\text{H}^{\theta}_{800\ ^{\circ}\text{C}} = 153.33\ \text{kJ/mol}$ | (4) |
| | $\text{C}_3\text{H}_6\text{O} + 5\text{H}_2\text{O} \rightarrow 3\,\text{CO}_2 + 8\text{H}_2,\ \Delta\text{H}^{\theta}_{800\ ^{\circ}\text{C}} = 295.90\ \text{kJ/mol}$ | (5) |
| | $\text{C}_6\text{H}_6\text{O} + 11\text{H}_2\text{O} \rightarrow 6\,\text{CO}_2 + 14\text{H}_2,\ \Delta\text{H}^{\theta}_{800\ ^{\circ}\text{C}} = 473.68\ \text{kJ/mol}$ | (6) |
| | $\text{CH}_4 + 2\text{H}_2\text{O} \rightarrow \text{CO}_2 + 4\text{H}_2,\ \Delta\text{H}^{\theta}_{800\ ^{\circ}\text{C}} = 191.10\ \text{kJ/mol}$ | (7) |
| Methanation reactions | $\text{C} + 2\text{H}_2 \rightarrow \text{CH}_4,\ \Delta\text{H}^{\theta}_{800\ ^{\circ}\text{C}} = -89.45\ \text{kJ/mol}$ | (8) |
| | $\text{CO} + 3\text{H}_2 \rightarrow \text{CH}_4 + \text{H}_2\text{O},\ \Delta\text{H}^{\theta}_{800\ ^{\circ}\text{C}} = -225.22\ \text{kJ/mol}$ | (9) |
| Water gas reaction | $\text{C} + \text{H}_2\text{O} \rightarrow \text{CO} + \text{H}_2,\ \Delta\text{H}^{\theta}_{800\ ^{\circ}\text{C}} = 135.77\ \text{kJ/mol}$ | (10) |
| Water gas shift reaction | $\text{CO} + \text{H}_2\text{O} \rightarrow \text{H}_2 + \text{CO}_2,\ \Delta\text{H}^{\theta}_{800\ ^{\circ}\text{C}} = -34.12\ \text{kJ/mol}$ | (11) |
| Bell reaction | $2\,\text{CO} \rightarrow \text{C} + \text{CO}_2,\ \Delta\text{H}^{\theta}_{800\ ^{\circ}\text{C}} = -169.88\ \text{kJ/mol}$ | (12) |

**Table 2.** *Cont.*

| Name | Equations | No. |
| --- | --- | --- |
| Reactions of mineral oxide with the generated gases | $CaO + CO_2 \rightarrow CaCO_3,\ \Delta H^{\theta}_{800\ ^{\circ}C} = -167.62\ kJ/mol$ | (13) |
| | $CaO + H_2O \rightarrow Ca(OH)_2,\ \Delta H^{\theta}_{800\ ^{\circ}C} = -61.88\ kJ/mol$ | (14) |
| | $Fe_2O_3 + H_2 \rightarrow 2FeO + H_2O,\ \Delta H^{\theta}_{800\ ^{\circ}C} = 28.89\ kJ/mol$ | (15) |
| | $Fe_2O_3 + CO \rightarrow 2FeO + CO_2,\ \Delta H^{\theta}_{800\ ^{\circ}C} = -5.23\ kJ/mol$ | (16) |
| | $4\,Fe_2O_3 + CH_4 \rightarrow 8FeO + CO_2 + 2H_2O,\ \Delta H^{\theta}_{800\ ^{\circ}C} = 306.64\ kJ/mol$ | (17) |
| | $1.132\,Fe_2O_3 + H_2 \rightarrow 2.395\,Fe_{0.945}O + H_2O,\ \Delta H^{\theta}_{800\ ^{\circ}C} = 40.95\ kJ/mol$ | (18) |
| | $1.132\,Fe_2O_3 + CO \rightarrow 2.395\,Fe_{0.945}O + CO_2, \Delta H^{\theta}_{800\ ^{\circ}C} = 6.84\ kJ/mol$ | (19) |
| | $4.527\,Fe_2O_3 + CH_4 \rightarrow 9.581\,Fe_{0.945}O + CO_2 + 2H_2O,\ \Delta H^{\theta}_{800\ ^{\circ}C} = 353.978\ kJ/mol$ | (20) |
| | $Fe_2O_3 + 3H_2 \rightarrow 2Fe + 3H_2O,\ \Delta H^{\theta}_{800\ ^{\circ}C} = 63.356\ kJ/mol$ | (21) |
| | $Fe_2O_3 + 3\,CO \rightarrow 2Fe + 3\,CO_2,\ \Delta H^{\theta}_{800\ ^{\circ}C} = -38.99\ kJ/mol$ | (22) |
| | $1.333\,Fe_2O_3 + CH_4 \rightarrow 2.667\,Fe + CO_2 + 2H_2O,\ \Delta H^{\theta}_{800\ ^{\circ}C} = 275.35\ kJ/mol$ | (23) |

### *2.3. Thermodynamic Methodology*

The process of catalyst-enhanced steam reforming of bio-oil to recover waste heat from granulated BF slag is complex and contains coupled chemical reaction mechanisms [38]. Choosing an appropriate method to evaluate the thermodynamic process of catalyst-enhanced steam reforming is the requirement of this study. Compared with the traditional thermodynamic calculation method of equilibrium constant and positive and reverse reaction rate, the minimum Gibbs free energy method could obtain reaction equilibrium productions simply mastering the materials before and after reactions [44,45] and is widely applied in thermodynamic calculation [45–47]. This paper applies the minimum Gibbs free energy method using HSC 6.0 software (Outokumpu Company, Finland compile) to obtain the equilibrium production. The potential gaseous and solid components of the process of catalyst-enhanced steam reforming of bio-oil to recover waste heat from granulated BF slag are illustrated in a previous study [30].

The thermodynamic calculation of the catalyst-enhanced steam reforming reaction in granulated BF slag is illustrated as follows [44,45]:

The total Gibbs free energy of the catalyst-enhanced steam reforming reaction ($G$) could be obtained from Equation (24).

$$G = \sum_{i=1}^{N} n_i \mu_i,\ i = 1,\ 2,\ 3,\ \ldots\ldots,\ N \tag{24}$$

In Equation (24), $n_i$ and $\mu_i$ represent the ratio amount of substance of matter specie and chemical potential (kJ/mol), respectively. The minimum $G$ is obtained when the catalyst-enhanced steam reforming process reaches thermodynamic balance.

The optimal $n_i$ obtained via the Lagrange multiplier is shown as follows:

$$\sum_{i=1}^{N} a_{ij} n_i = A_j,\ j = 1,\ 2,\ 3,\ \ldots\ldots,\ M \tag{25}$$

In Equation (25), $a_{ij}$ and $A_j$ represent the total number of $j_{th}$ element in the $i_{th}$ matter specie and the total number of $j_{th}$ element in the catalyst-enhanced steam reforming reaction, respectively. Additionally, the principle of the Lagrange multiplier ($L$) is shown as follows:

$$L = \sum_{i=1}^{N} n_i \mu_i - \sum_{j=i}^{M} \lambda_j \left( \sum_{i=1}^{N} (a_{ij} n_i - A_j) \right) \quad (26)$$

In Equation (26), $\lambda_j$ represents the Lagrange multiplier of the $j_{th}$ element in the catalyst-enhanced steam reforming reaction. When the Gibbs free energy reaches the maximum value, the differential coefficient of $L$ is equal to 0. The calculation process is shown as follows:

$$\frac{\partial L}{\partial n_i} = \mu_i - \sum_{j=1}^{M} \lambda_j a_{ji} = 0 \quad (27)$$

The product distributions of catalyst-enhanced steam reforming reaction could be obtained via Equation (27).

### *2.4. Evaluation Parameters*

In order to obtain the optimal conditions of catalyst-enhanced steam reforming of bio-oil in granulated BF slag, the evaluation parameters are hydrogen yield, carbonaceous productions and gas concentration.

Hydrogen yield: The hydrogen production is the main parameter during the evaluation of the process of hydrogen production from catalyst-enhanced steam reforming over granulated BF as heat carrier. The hydrogen yield is defined as follows:

$$\text{Hydrogen yield} = \frac{\text{moles of } H_2 \text{ in the production}}{\text{mole of theoretical } H_2 \text{ production}} \times 100\% \quad (28)$$

In Equation (28), the mole of theoretical $H_2$ production is the maximum $H_2$ production when the catalyst-enhanced steam reforming reaction is complete.

Carbonaceous productions: The carbonaceous productions (containing CO production, $CH_4$ production and coke production) are also obtained via the steam reforming process. The carbonaceous production is defined as follows:

$$\text{Carbonaceous production} = \frac{\text{moles of CO } (CH_4,\ CO_2 \text{ or C}) \text{ in the production}}{\text{kg of bio-oil}} \quad (29)$$

Gas concentration: The gas concentrations ($H_2$ concentration, CO concentration and CH4 concentration) are defined as follows:

$$\text{Gas concentration} = \frac{\text{moles of } H_2(\text{CO and } CH_4) \text{ in the production}}{\text{total moles of dry reformed gas}} \times 100\% \quad (30)$$

## 3. Results and Discussion

### *3.1. The Effects of Temperature*

The process of catalyst-enhanced steam reforming in granulated BF slag is an endothermic process. Additionally, the irregular motion of molecules intensifies with the increasing temperature [23,43]. The temperature significantly effects the process of catalyst-enhanced steam reforming.

Figure 1 shows the hydrogen yield of the catalyst-enhanced steam reforming process under different temperatures and S/C at the pressure of 1 bar. From Figure 1, when the S/C is zero, only the catalyst-enhanced decomposition of bio-oil occurs in the process of recovery waste heat from granulated BF slag. The hydrogen yield increases with the increasing temperature. When the S/C is zero, the endothermic thermal cracking reaction (Equation (1)), water gas reaction (Equation (10)) and the exothermal methanation reactions

(Equations (8) and (9)) are the primary reactions of catalyst-enhanced bio-oil decomposition. According to Le Chatelier's principle, the endothermic reactions (Equations (1) and (10)) shift to the right side and the exothermal reactions (Equations (8) and (9)) shift to the left side with the increasing temperature, increasing the hydrogen yield. Also from Figure 1, when the S/C is higher than one, the catalyst-enhanced steam reforming of bio-oil occurs in the process of recovery waste heat from granulated BF slag. The hydrogen yield first increases and then decreases with the increasing temperature. Taking the S/C of three, for example, the hydrogen yield increases from 5.94% to 83.85% with the temperature increasing from 200 °C to 690 °C, and it decreases from 83.85% to 75.55% with the temperature increasing from 690 °C to 1000 °C. The process of catalyst-enhanced steam reforming of bio-oil is an endothermic process. But as the S/C increases, at high temperatures, the water gas shift reaction (Equation (11)) could affect the process of catalyst-enhanced steam reforming of bio-oil gradually. According to Le Chatelier's principle, the exothermal water gas shift reaction (Equation (11)) shifts to the left side with the increasing temperature, decreasing the hydrogen yield. Xie investigated the hydrogen production from steam reforming of raw coke oven gas via thermodynamic analysis [46,48]. The results implied that when the S/C is higher than two, the hydrogen yield first increases then decreases with the increasing temperature [46].

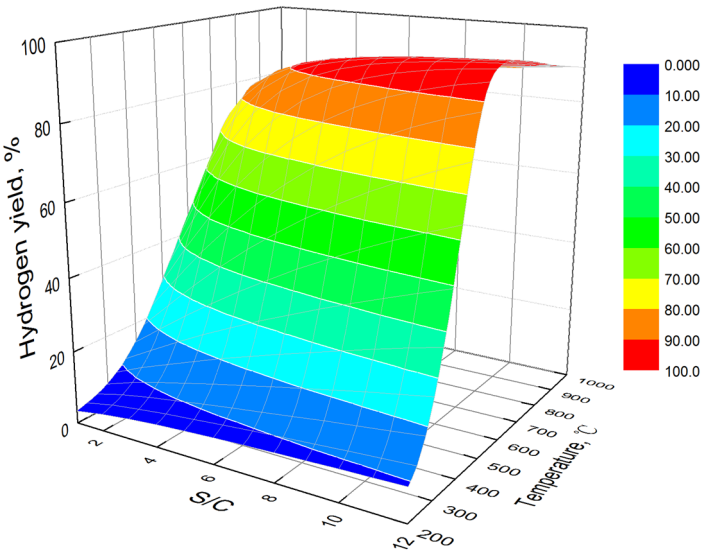


**Figure 1.** The hydrogen yield of catalyst-enhanced steam reforming under different temperatures and S/C (pressure of 1 bar; mass ratio of catalyst:slag:bio-oil of 1:1:1).

Figure 2 shows the carbon monoxide production of a catalyst-enhanced steam reforming reaction under different temperatures and S/C at the pressure of 1 bar. From Figure 2, under different S/C, the carbon monoxide production shows a similar variation with the increasing temperature. Taking the S/C of four for example, when the temperature is lower than 300 °C, the carbon monoxide production is almost zero during the process of catalyst-enhanced steam reforming to recover waste heat from BF slag. The results imply that the thermal cracking reaction (Equation (1)) and water gas reaction (Equation (10)) hardly proceed at low temperatures. When the temperature is higher than 300 °C, the carbon monoxide production increases with the increasing temperature. The maximum carbon monoxide production is 25.44 mol/kg at the temperature of 1000 °C. According to Le Chatelier's principle, the endothermic reactions of the thermal cracking reaction (Equation (1)) and water gas reaction (Equation (10)) shift to the right side, and the exothermal reactions of water gas shift reaction (Equation (11)) and Bell reaction (Equation (12)) shift to the left side with the increasing temperature, increasing carbon monoxide production. The experiments of bio-oil steam reforming were carried out in fixed bed and the carbon monoxide increased with the increasing temperature [37].

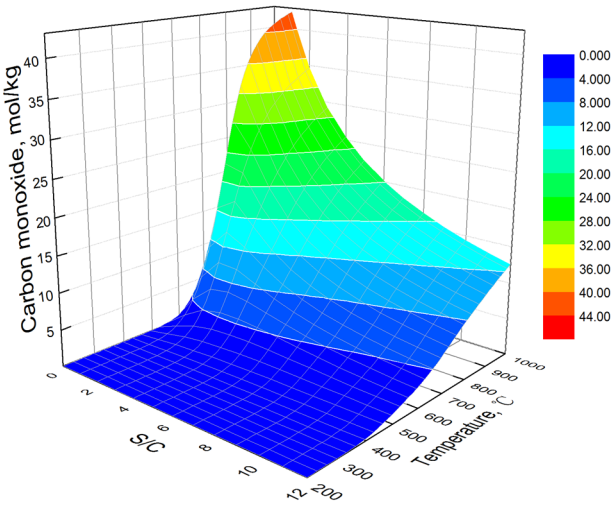


**Figure 2.** The carbon monoxide production of catalyst-enhanced steam reforming under different temperatures and S/C (pressure of 1 bar; the mass ratio of catalyst:slag:bio-oil of 1:1:1).

Figure 3 shows the methane production of catalyst-enhanced steam reforming reaction under different temperatures and S/C at the pressure of 1 bar. From Figure 3, under different S/C, the methane production shows a similar variation with the increasing temperature. Taking the S/C of five for example, the methane production is 25.44 mol/kg at the temperature of 200 °C. The methane production decreases with the increasing temperature and it is almost zero at the temperature of 820 °C. According to Le Chatelier's principle, the endothermic reaction of methane steam reforming (Equation (7)) shifts to the right side and the exothermal reactions of methanation (Equations (8) and (9)) shift to the left side with the increasing temperature, decreasing the methane production. The increasing temperature was adverse to methane production, which was also obtained via the process of steam reforming of simulated bio-oil over Ce-Ni/Co catalyst [49].

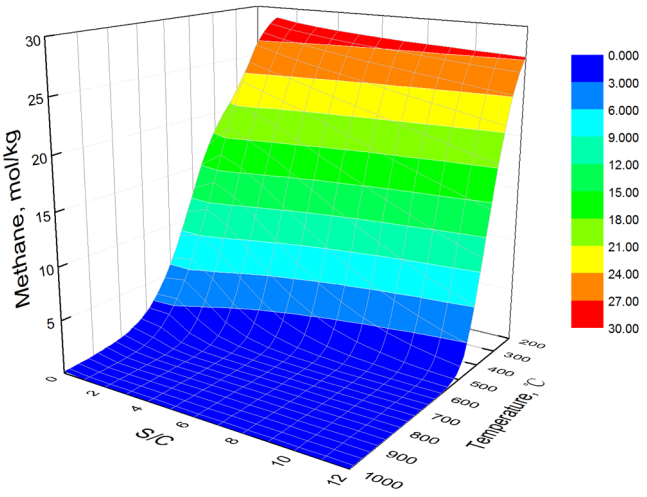


**Figure 3.** The methane production of catalyst-enhanced steam reforming under different temperatures and S/C (pressure of 1 bar; mass ratio of catalyst:slag:bio-oil of 1:1:1).

Figure 4 shows the carbon dioxide production of the catalyst-enhanced steam reforming reaction under different temperatures and S/C at the pressure of 1 bar. From Figure 4, under different S/C, the carbon dioxide production shows a similar variation with the increasing temperature. Taking the S/C of five for example, the carbon dioxide production first increases and then decreases with the increasing temperature. The carbon dioxide production increases from 0.02 mol/kg to 29.32 mol/kg with the temperature increasing

from 200 °C to 780 °C and decreases from 29.32 mol/kg to 25.41 mol/kg with the temperature increasing from 780 °C to 1000 °C. At low temperatures, the endothermic reactions of thermal cracking (Equations (1) and (2)), steam reforming (Equations (3)–(7)), mineral oxide with the generated gases (Equations (17) and (19)) and the exothermal reaction of mineral oxide with the generated gases (Equation (13)) are the primary reactions during the process of catalyst-enhanced steam reforming to recover waste heat from granulated BF slag. According to Le Chatelier's principle, the endothermic reactions (Equations (1)–(7), (17) and (19)) shift to the right side and the exothermal reaction (Equation (13)) shift to the left side with the increasing temperature, increasing carbon dioxide production. At high temperatures, the exothermal reactions of water gas shift (Equation (11)), Bell reaction (Equation (12)) and mineral oxide with the generated gases (Equations (16) and (22)) are the primary reactions during the process of catalyst-enhanced steam reforming to recover waste heat from granulated BF slag. According to Le Chatelier's principle, these exothermal reactions shift to the left side with the increasing temperature, decreasing carbon dioxide production. The variation of carbon dioxide production was similar to the steam reforming of bio-oil model compounds in granulated BF slag [30].

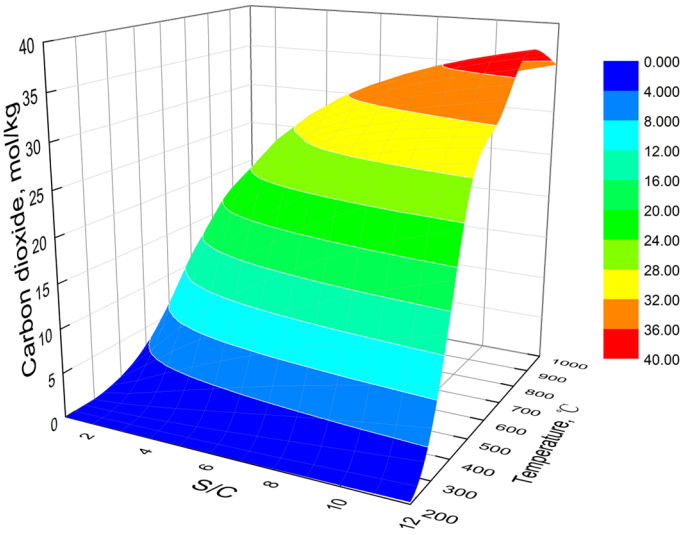


**Figure 4.** The carbon dioxide production of catalyst-enhanced steam reforming under different temperatures and S/C (pressure of 1 bar; mass ratio of catalyst:slag:bio-oil of 1:1:1).

Figure 5 shows the hydrogen concentration of the catalyst-enhanced steam reforming reaction under different temperatures and S/C at the pressure of 1 bar. From Figure 5, under different S/C, the hydrogen concentration shows a similar variation with the increasing temperature. Taking the S/C of five, for example, the hydrogen concentration first increases and then decreases with the increasing temperature. The hydrogen concentration increases from 22.47% to 76.85% with the temperature increasing from 200 °C to 575 °C, and it decreases from 76.85% to 67.21% with the temperature increasing from 575 °C to 1000 °C. When the S/C is zero, the hydrogen yield increases with the increasing temperature, but carbon monoxide production increases further at high temperatures, decreasing the hydrogen concentration. When the S/C is higher than one, the variation trend of hydrogen concentration is similar to that of hydrogen yield. When the catalyst-enhanced steam reforming of bio-oil reaction occurs in the process of recovery waste heat from granulated BF slag, the hydrogen yield is the primary influence factor of the hydrogen concentration.

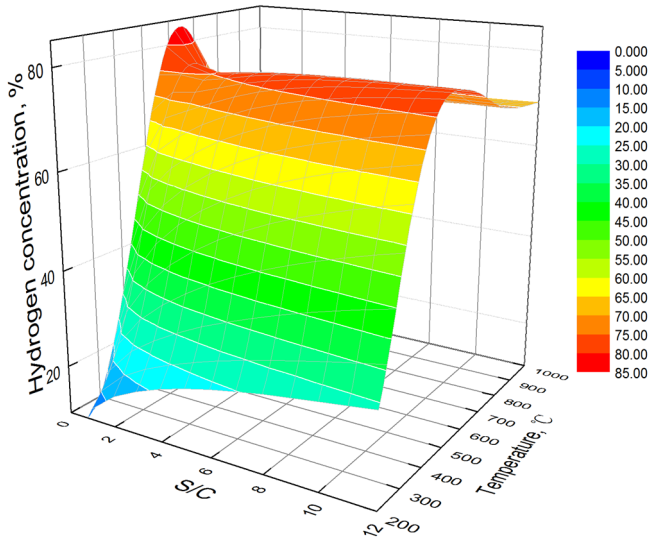


**Figure 5.** The hydrogen concentration of catalyst-enhanced steam reforming under different temperatures and S/C (pressure of 1 bar; mass ratio of catalyst:slag:bio-oil of 1:1:1).

Figure 6 shows the carbon monoxide concentration of the catalyst-enhanced steam reforming reaction under different temperatures and S/C at the pressure of 1 bar. From Figure 6, the carbon monoxide concentration increases with the increasing temperature. Taking the S/C of five, for example, the carbon monoxide concentration increases from 0 to 15.4% with the temperature increasing from 200 °C to 1000 °C. From Figure 2, the carbon monoxide production also increases with the increasing temperature. These results imply that carbon monoxide concentration is mainly dependent on the carbon monoxide production during the process of catalyst-enhanced reforming to recover waste heat from granulated BF slag.

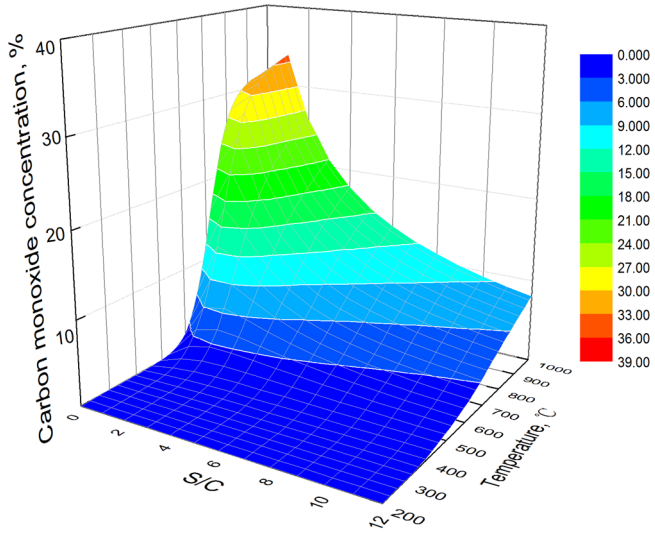


**Figure 6.** The carbon monoxide concentration of catalyst-enhanced steam reforming under different temperatures and S/C (pressure of 1 bar; mass ratio of catalyst:slag:bio-oil of 1:1:1).

Figure 7 shows the methane concentration of the catalyst-enhanced steam reforming reaction under different temperatures and S/C at the pressure of 1 bar. From Figure 8, the methane concentration decreases with the increasing temperature. Taking the S/C of four, for example, the methane concentration is 79.1% at the temperature of 200 °C and it is close to 0 at the temperature of 625 °C. At low temperatures, the hydrogen yield, carbon monoxide production and carbon dioxide production increase with the increasing temperature.

Additionally, methane production decreases with the increasing temperature. These factors result that the methane concentration decreases with the increasing temperature. At high temperatures, the methane production decreases with the increasing temperature, which is regarded as the main factor of variations in the methane concentration.

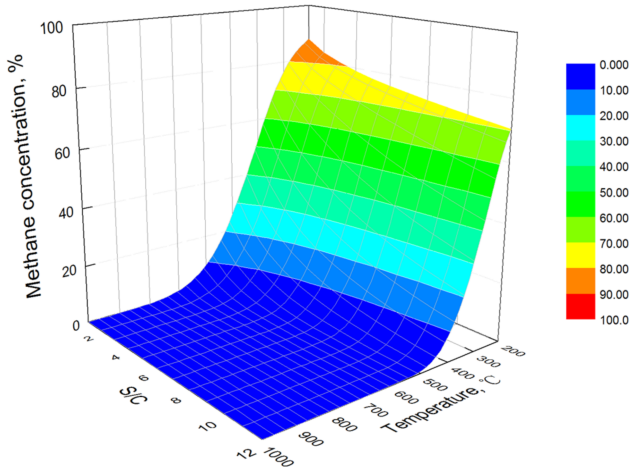


**Figure 7.** The methane concentration of catalyst-enhanced steam reforming under different temperatures and S/C (pressure of 1 bar; mass ratio of catalyst:slag:bio-oil of 1:1:1).

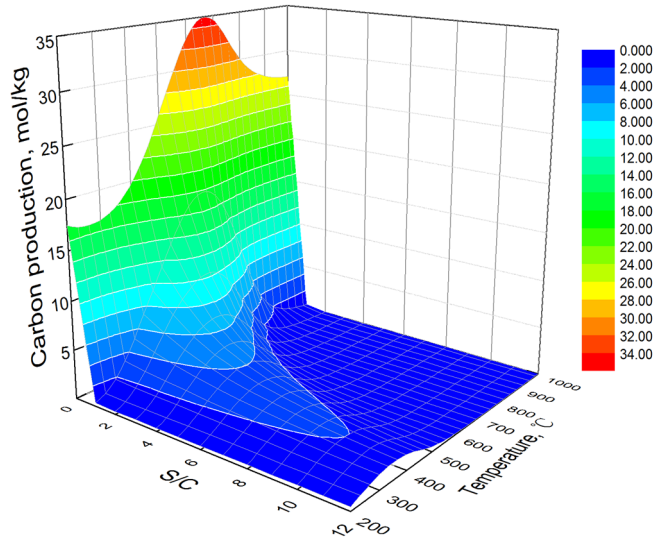


**Figure 8.** The carbon production of catalyst-enhanced steam reforming under different temperatures and S/C (pressure of 1 bar; mass ratio of catalyst:slag:bio-oil of 1:1:1).

Carbon can be formatted from the process of catalyst-enhanced steam reforming recovery waste heat from granulated BF slag [37]. The carbon could affect the contact of the bio-oil, slag and catalyst, which is not conducive to heat and mass transfer of the process of steam reforming. Additionally, carbon affects the catalyst activity [50]. Carbon formation could affect the process of catalyst-enhanced steam reforming to recover waste heat from granulated BF slag in industrial production. Carbon formation under different temperatures, S/C, pressure and catalysts is performed in this paper.

Figure 8 shows the carbon production of a catalyst-enhanced steam reforming reaction under different temperatures and S/C at the pressure of 1 bar. From Figure 9, the carbon production first increases and then decreases with the increasing temperature. Taking the S/C of four, for example, carbon production increases from 0.33 mol/kg to 5.09 mol/kg with the temperature increasing from 200 °C to 445 °C and decreases from 5.09 mol/kg to 0.01 mol/kg with the temperature increasing from 445 °C to 1000 °C. At low temperatures,

the endothermic thermal cracking reaction (Equation (1)) and exothermic methanation reaction (Equation (8)) are the main reactions affecting carbon production. According to Le Chatelier's principle, the endothermic thermal cracking reaction shifts to the right side and the exothermic methanation reaction shifts to the left side with the increasing temperature, increasing carbon production. But at high temperatures, the endothermic water gas reaction (Equation (10)) and the exothermic Bell reaction (Equation (12)) are the main reactions affecting carbon production. According to Le Chatelier's principle, the endothermic water gas reaction shifts to the right side and the exothermic Bell reaction shifts to the left side with increasing temperature, decreasing the carbon production.

### 3.2. The Effects of S/C

The H-O bond in steam would be broken and the C-O bond and H-H bond would be recombined during the process of catalyst-enhanced steam reforming in granulated BF slag. The quantity of steam has significant effects on the product distribution of the catalyst-enhanced steam reforming process [30,47].

The effects of S/C on the hydrogen yield of the catalyst-enhanced steam reforming reaction are also shown in Figure 1. From Figure 1, the hydrogen yield increases with the increasing S/C. Taking the temperature of 700 °C, for example, the hydrogen yield increases from 29.89% to 95.76% with the S/C increasing from 0 to 12. The steam reforming reactions (Equations (2)–(7)), water gas reaction (Equation (10)) and water gas shift reaction (Equation (11)) would shift to the right side, and the methanation reaction (Equation (9)) and the reactions of mineral oxide with the generated gases (Equations (15), (18) and (21)) would shift to the left side, increasing the hydrogen yield. Increasing S/C was beneficial for hydrogen yield, which was also obtained via the process of steam reforming of tar [50].

The effects of S/C on the carbon monoxide production of catalyst-enhanced steam reforming reactions are also shown in Figure 2. From Figure 2, at low temperatures (lower than 420 °C), the carbon monoxide production increases with the increasing S/C. Taking the temperature of 380 °C for example, the carbon monoxide production increases from 0 mol/kg to 0.13 mol/kg with the S/C increasing from 0 to 12. But at high temperatures (higher than 420 °C), the carbon monoxide production first increases and then decreases with the increasing S/C. Taking the temperature of 690 °C for example, the carbon monoxide production increases from 4.83 mol/kg to 17.98 mol/kg with the S/C increasing from 0 to 2 and it decreases from 17.98 mol/kg to 5.76 mol/kg with the S/C increasing from 2 to 12. At low temperatures, the methanation reaction (Equation (9)) and water gas reaction (Equation (10)) are the main reactions affecting carbon monoxide production. With increasing S/C, the methanation reaction and water gas reaction shift to the left side and right side, respectively, increasing the carbon monoxide production. At high temperatures and low S/C, the carbon monoxide production increases with the increasing S/C. But at high temperatures and high S/C, the water gas shift reaction (Equation (11)) is the main reaction affecting carbon monoxide production. With the increasing S/C, the water gas shift reaction shifts to the right side, decreasing the carbon monoxide production.

The effects of S/C on the methane production of catalyst-enhanced steam reforming reaction are also shown in Figure 3. From Figure 3, at low temperatures (lower than 673 °C), the methane production first increases and then decreases with the increasing S/C. Taking the temperature of 396 °C, for example, the methane production increases from 18.45 mol/kg to 21.14 mol/kg with the S/C increasing from 0 to 1 and it decreases from 21.14 mol/kg to 10.20 mol/kg with the S/C increasing from 1 to 12. But at high temperatures (higher than 673 °C), the methane production decreases with the increasing S/C. Taking the temperature of 804 °C for example, the methane production decreases from 0.77 mol/kg to 0 mol/kg with the S/C increasing from 0 to 12. At low temperatures and low S/C, the methanation reaction (Equation (9)) is the main reaction affecting methane production and shifts to the left side, increasing the methane production. But at low temperatures and high S/C, or high temperatures, the methane reforming reaction (Equation (7))

is the main reaction affecting methane production and shifts to the right side, decreasing the methane production.

The effects of S/C on the carbon dioxide production of the catalyst-enhanced steam reforming of bio-oil are also shown in Figure 4. From Figure 4, the carbon dioxide production increases with the increasing S/C. Taking the temperature of 657 °C, for example, the carbon dioxide production increases from 0.65 mol/kg to 33.99 mol/kg with the S/C increasing from 0 to 12. With the increasing S/C, the steam reforming reactions (Equations (2)–(7)) and water gas shift reaction (Equation (11)) shift to the right side, increasing the carbon dioxide production.

The effects of S/C on the hydrogen concentration, carbon monoxide concentration and methane concentration of the catalyst-enhanced steam reforming reaction are also shown in Figures 5–7, respectively. From Figure 5, at low temperatures (lower than 559 °C), the hydrogen concentration increases with the increasing S/C. Taking temperature of 445 °C for example, the hydrogen concentration increases from 43.56% to 76.72% with the S/C increasing from 0 to 12. The variations of hydrogen concentration are attributed to the increasing hydrogen yield. But at high temperatures (higher than 559 °C), the hydrogen concentration first decreases and then increases with the increasing S/C. Taking the temperature of 837 °C, for example, the hydrogen concentration decreases from 69.21% to 63.47% with the S/C increasing from 0 to 1 and increases from 63.47% to 70.42% with the S/C increasing from 1 to 12. At high temperatures, the hydrogen concentration is the lowest, and the carbon monoxide production is also the lowest at the S/C of zero, resulting that the hydrogen concentration is not lowest with the S/C of zero. From Figure 6, at low temperatures, the carbon monoxide concentration is almost zero. At high temperatures, the carbon monoxide concentration first increases and then decreases with the increasing S/C. The variation trend of carbon monoxide concentration is mainly attributable to the carbon monoxide production. From Figure 7, the methane concentration decreases with the increasing S/C. At low temperatures and low S/C, the methane production, hydrogen yield and carbon monoxide production increase with the increasing S/C. These factors result that the methane concentration decreases with the increasing S/C. At low temperatures and high S/C, or high temperatures, the methane production decreased, resulting that the methane concentration decreases with the increasing S/C.

The effects of S/C on the carbon production of catalyst-enhanced steam reforming reaction are also shown in Figure 8. From Figure 8, the carbon production decreases with the increasing S/C. Taking the temperature of 657 °C, for example, the carbon production decreases from 34.92 mol/kg to 0.04 mol/kg with the S/C increasing from 0 to 12. With the increasing S/C, the water gas reaction (Equation (10)) is the main reaction affecting carbon production and shifts to the right side, decreasing the carbon production.

### *3.3. The Effects of Pressure*

The reaction pressure might affect the partial pressure of reactants and products [30,44,51], which could have significant effects on the product distribution of catalyst-enhanced steam reforming process.

Figure 9 shows the hydrogen yield of catalyst-enhanced steam reforming reaction under different temperatures and pressures with the S/C of eight. From Figure 9, at low temperatures (lower than 600 °C), the hydrogen yield decreases with the increasing pressure. Taking the temperature of 600 °C for example, the hydrogen yield decreases from 95.25% to 76.06% with the pressure increasing from 0.01 bar to 10 bar. During the process of catalyst-enhanced steam reforming, the thermal cracking reaction (Equation (1)), steam reforming reactions (Equations (2)–(7)), methanation reaction (Equations (8) and (9)), water gas reaction (Equation (10)) are the primary reactions affecting the hydrogen yield. According to Le Chatelier's principle, the thermal cracking reaction (Equation (1)), steam reforming reactions (Equations (2)–(7)) and water gas reaction (Equation (10)) shift to the left side and methanation reaction (Equations (8) and (9)) shifts to the right side with the increasing pressure, decreasing the hydrogen yield. But at high temperatures (higher than

600 °C), the pressure has a little effects on the hydrogen yield. Taking the temperature of 900 °C for example, the hydrogen yield is from 87.95% to 88.59% with the pressure increasing from 0.01 bar to 10 bar. The increasing pressure was adverse to the hydrogen production, which was also obtained from the process of bio-oil steam reforming [51].

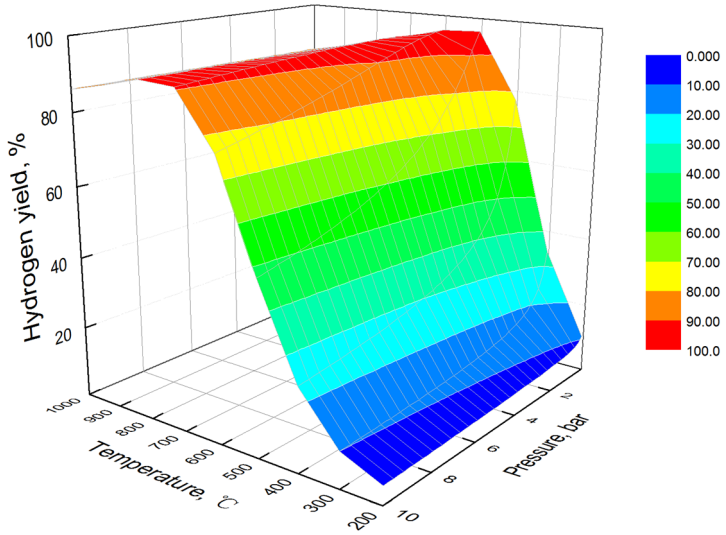


**Figure 9.** The hydrogen yield of catalyst-enhanced steam reforming under different temperatures and pressures (S/C of eight; mass ratio of catalyst:slag:bio-oil of 1:1:1).

Figure 10 shows the carbon monoxide production of catalyst-enhanced steam reforming reaction under different temperatures and pressures with the S/C of eight. From Figure 10, the carbon monoxide production decreases with the increasing pressure. Taking the temperature of 700 °C for example, the carbon monoxide production decreases from 8.73 mol/kg to 5.97 mol/kg with the pressure decreasing from 0.01 bar to 10 bar. During the process of catalyst-enhanced steam reforming, the methanation reaction (Equation (9)), water gas reaction (Equation (10)) and Bell reaction (Equation (12)) are the primary reactions affecting the carbon monoxide production. According to Le Chatelier's principle, the methanation reaction and Bell reaction shift to the right side, and the water gas reaction shifts to the left side, decreasing the carbon monoxide production.

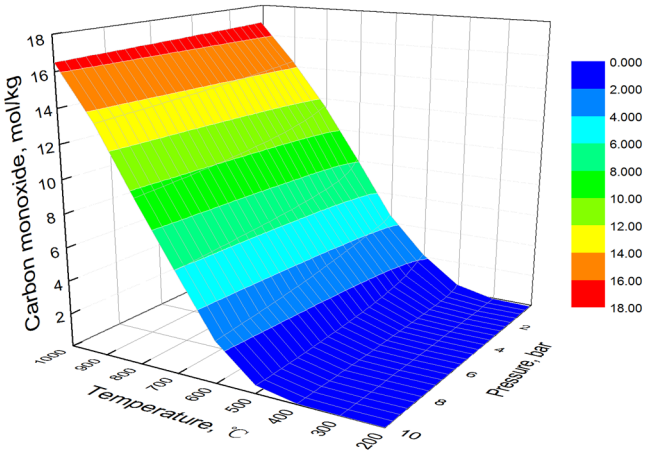


**Figure 10.** The carbon monoxide production of catalyst-enhanced steam reforming under different temperatures and pressures (S/C of eight; mass ratio of catalyst:slag:bio-oil of 1:1:1).

Figure 11 shows the methane production of catalyst-enhanced steam reforming reaction under different temperatures and pressures with the S/C of eight. From Figure 11, the methane production increases with the increasing pressure. Taking the temperature of

500 °C for example, the methane production increases from 0 mol/kg to 14.66 mol/kg with the pressure increasing from 0.01 bar to 10 bar. During the process of catalyst-enhanced steam reforming, the methane reforming reaction (Equation (7)) and methanation reactions (Equations (8) and (9)) are the primary reactions affecting the methane production. According to Le Chatelier's principle, the methane reforming reaction shifts to the left side and the methanation reactions shifts to the right side, increasing the methane production.

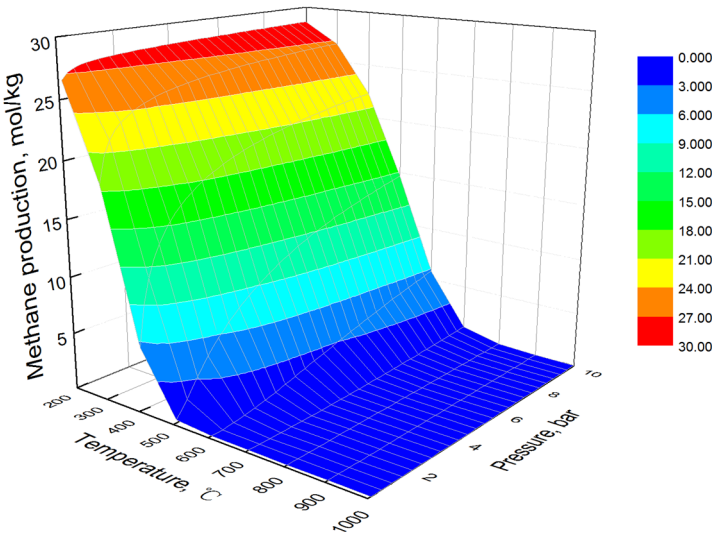


**Figure 11.** The methane production of catalyst-enhanced steam reforming under different temperatures and pressures (S/C of eight; mass ratio of catalyst:slag:bio-oil of 1:1:1).

The hydrogen concentration, carbon monoxide concentration and methane concentration of catalyst-enhanced steam reforming reaction under different temperatures and pressures with the S/C of eight are shown in Figures 12–14, respectively. From these figures, at low temperatures (lower than 600 °C), the hydrogen concentration shows a decreasing trend but methane concentration shows an increasing trend with the increasing pressure (higher than 600 °C). These variations are similar to their yield. At high temperatures, the hydrogen concentration and methane concentration are almost unchanged with the increasing pressure. The carbon monoxide concentration is almost unchanged with the increasing pressure. The results imply that the variation in carbon monoxide production and the variations in hydrogen concentration and methane concentration at high temperatures are similar to the variation in syngas production.

Figure 15 shows the carbon production of catalyst-enhanced steam reforming reaction under different temperatures and pressures with the S/C of eight. From Figure 15, at low temperatures (lower than 300 °C), the carbon production decreases with the increasing pressure. Taking the temperature of 300 °C for example, the carbon production decreases from 2.25 mol/kg to 0.86 mol/kg with the pressure increasing from 0.01 bar to 10 bar. At low temperatures, the methanation reaction (Equation (8)) is the primary reaction affecting the carbon production and shifts to the right side with the increasing pressure, increasing the carbon production. At high temperatures (higher than 300 °C), the carbon production increases with the increasing pressure. Taking the temperature of 700 °C for example, the carbon production increases from 0.00 mol/kg to 0.63 mol/kg with the pressure increasing from 0.01 bar to 10 bar. At high temperatures, the thermal cracking reaction (Equation (1)), water gas reaction (Equation (10)) and Bell reaction (Equation (12)) are the primary reactions affecting the carbon production. The thermal cracking reaction and Bell reaction shift to the right side and water gas reaction shifts to the left side with the increasing pressure, increasing the carbon production.

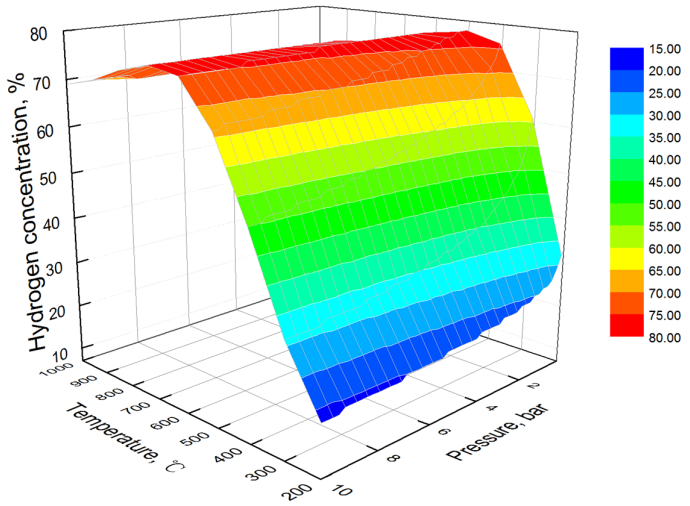


**Figure 12.** The hydrogen concentration of catalyst-enhanced steam reforming under different temperatures and pressures (S/C of eight; mass ratio of catalyst:slag:bio-oil of 1:1:1).

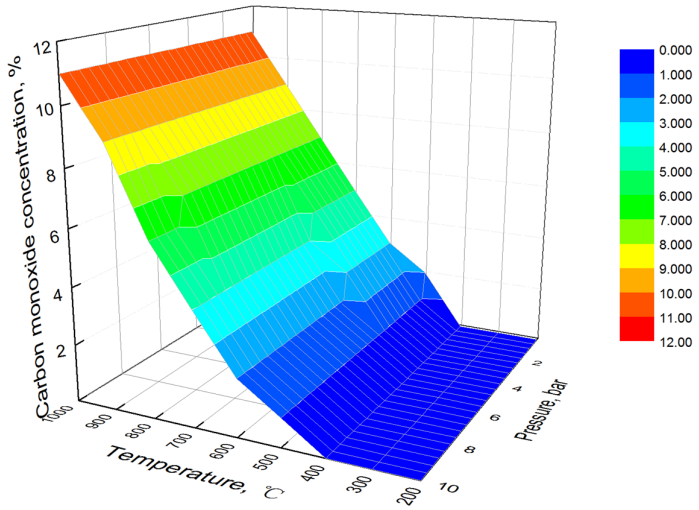


**Figure 13.** The carbon monoxide concentration of catalyst-enhanced steam reforming under different temperatures and pressures (S/C of eight; mass ratio of catalyst:slag:bio-oil of 1:1:1).

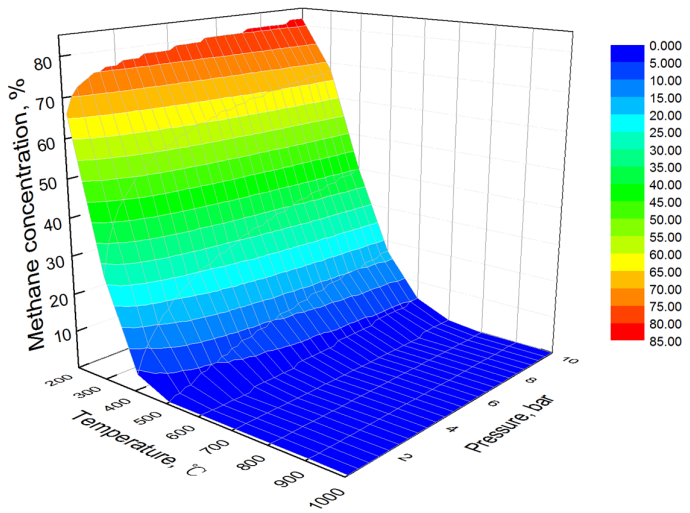


**Figure 14.** The methane concentration of catalyst-enhanced steam reforming under different temperatures and pressures (S/C of eight; mass ratio of catalyst:slag:bio-oil of 1:1:1).

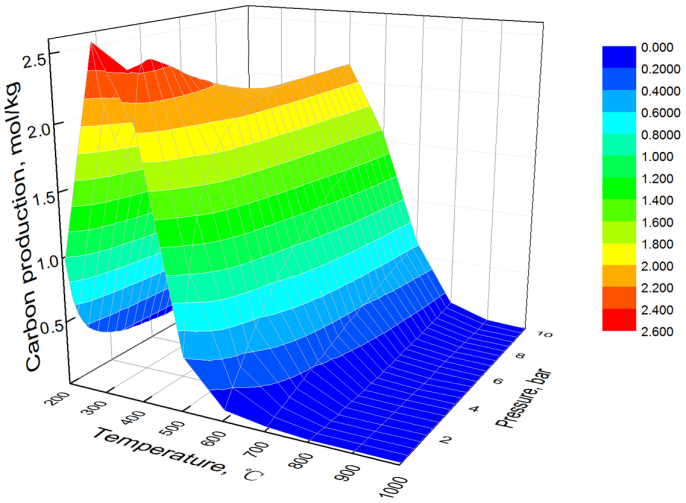


**Figure 15.** The carbon production of catalyst-enhanced steam reforming under different temperatures and pressures (S/C of eight; mass ratio of catalyst:slag:bio-oil of 1:1:1).

### *3.4. The Optimal Condition*

Coupled effects of temperature, S/C and pressure on the process of catalyst-enhanced steam reforming of bio-oil steam reforming are shown in Figures 1–16. The catalyst-enhanced steam reforming of bio-oil to recover waste heat from granulated BF slag is aimed at obtaining the hydrogen. The carbon has a remarkable effect on the heat and mass transfer and catalyst during the industrial production [37,50]. Thus, the hydrogen yield, hydrogen concentration and carbon production are regarded as the main factors for selecting the optimal condition.

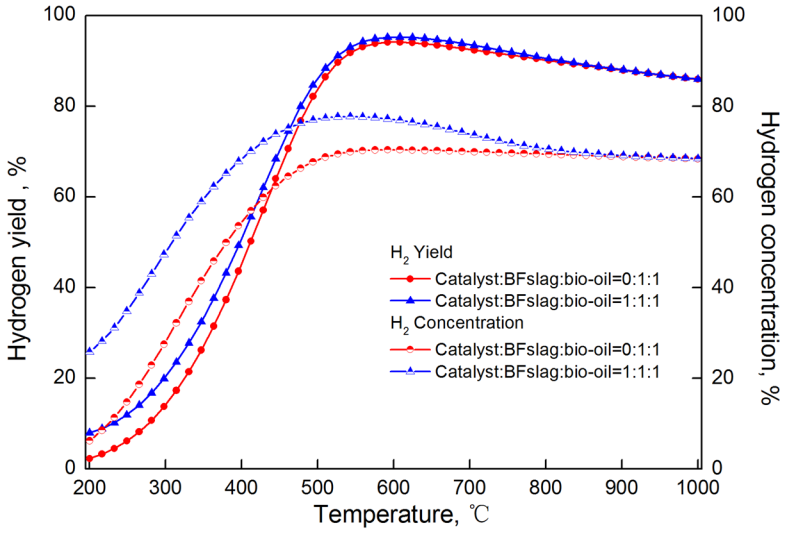


**Figure 16.** The hydrogen yield and hydrogen concentration of catalyst-enhanced steam reforming under different temperatures and carriers (S/C of eight and pressure of 1 bar).

From Section 3.1, Section 3.2, Section 3.3, when the S/C is eight, the maximal hydrogen yield is 95.25% at 608 °C. The hydrogen yield increases with the increasing S/C. But the maximal hydrogen yield is 97.32% with the S/C of 12. When S/C is higher than eight, the S/C has a pimping effect on the hydrogen yield. The increasing S/C could increase the energy consumption during the actual application process. In addition, when the S/C is eight and temperature is 608 °C, the hydrogen concentration is 76.89% and the carbon production is 0.28 mol/kg. The hydrogen concentration is close to the maximum concentration (77.72%) and the carbon production is close to zero at temperature of 608 °C and S/C of eight. Thus, the S/C of eight and temperature of 608 °C are regarded as the

optimal S/C and temperature, respectively. From Figure 9, at S/C of eight and temperature of 608 °C, the hydrogen yield shows an increasing trend with the increasing pressure. But at 1 bar, the hydrogen yield is closed to the maximum value, which is 95.71%. Meanwhile, the hydrogen concentration is close to the maximum value, which is 77.20%. The carbon production decreases with the increasing pressure, but it is close to 0 at 1 bar. The increasing pressure could increase the hydrogen yield and decrease the carbon production, which is beneficial for the process of catalyst-enhanced steam reforming of bio-oil to recover waste heat from granulated BF slag. But when the pressure is 1 bar, the hydrogen yield and the carbon production are closed to the optimal values and decreasing pressure could promote the equipment cost in the industrial application. Thus, the pressure of 1 bar is regarded as the optimal pressure during the process of catalyst-enhanced steam reforming of bio-oil to recover waste heat from granulated BF slag.

### *3.5. The Mechanism of Catalyst-Enhanced Steam Reforming*

The catalyst (CaO) [34–36] and granulated BF slag [30–32] could affect the product distribution of the bio-oil steam reforming process. The hydrogen yield, hydrogen concentration and carbon production are used as the main factors for evaluating the reforming process.

Figure 16 shows the hydrogen yield and hydrogen concentration of bio-oil steam reforming under different temperatures and carriers. From Figure 16, the catalyst could significantly increase the hydrogen yield and hydrogen concentration of bio-oil steam reforming in granulated BF slag. Taking the temperature of 625 °C, for example, the catalyst could improve the hydrogen yield and hydrogen concentration from 93.99% and 70.31% to 95.15% and 76.49%, respectively. The maximum hydrogen yield and hydrogen component are shown in Table 3. From Table 3, the maximum hydrogen yield and hydrogen component of the catalyst-enhanced steam reforming of bio-oil are higher than that of steam reforming of bio-oil. From the perspective of equilibrium calculation, the CaO could absorb $CO_2$ according to Equation (13), so it would be beneficial for the thermal cracking reaction (Equation (1)), steam reforming reactions (Equations (2)–(7)) and water gas shift reaction, increasing the hydrogen yield and hydrogen concentration. CaO could catalyze the process of bio-oil steam reforming and could be obtained via calcine calcium carbonate during the industry application [34–37,49]. In other words, catalyst-enhanced steam reforming of bio-oil using CaO as the catalyst could recover the waste heat from granulated BF slag with high hydrogen yield and hydrogen concentration.

**Table 3.** The maximum hydrogen yield and hydrogen component.

| Condition | Maximum Hydrogen Yield | Maximum Hydrogen Component |
|---|---|---|
| With catalyst | 95.30% | 77.73% |
| Without catalyst | 94.12% | 70.36% |

Figure 17 shows the carbon production of bio-oil steam reforming under different temperatures and carriers. From Figure 17, at low temperatures (lower than 265 °C), the carbon production is lower with the catalyst than without the catalyst. But at high temperatures, the carbon production is higher with the catalyst than without the catalyst. At low temperatures, the methanation reaction (Equation (8)) mainly affects carbon production. From Figure 17, the catalyst could increase the hydrogen yield, which could be beneficial for the methanation reaction (Equation (8)), decreasing carbon production. But at high temperatures, the thermal cracking reaction (Equation (1)), water gas reaction (Equation (10)) and Bell reaction (Equation (12)) mainly affect the carbon production. The catalyst could increase the hydrogen yield and decrease the carbon dioxide production, which could shift the thermal cracking reaction and Bell reaction to the right side and shift the water gas reaction to the left side, increasing the carbon production. At the optimal condition (the temperature of 608 °C, S/C of eight and pressure of 1 bar), the variation in carbon

production is not obvious with or without the catalyst. But at low temperatures (about 400 °C), the carbon production is obviously higher with the catalyst than without the catalyst. Using the catalyst-enhanced steam reforming of bio-oil to recover waste heat from granulated BF slag with the low temperatures, the negative effects of carbon production should be weakened via promotion of the performance of the catalyst, such as porosity or specific surface area [28,37].

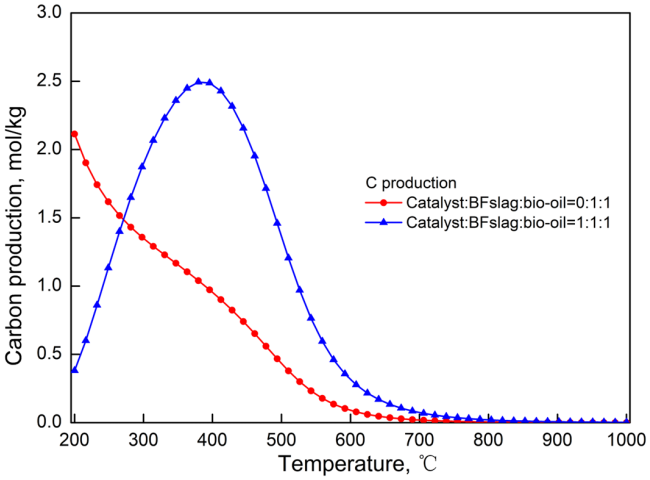


**Figure 17.** The carbon production of catalyst-enhanced steam reforming under different temperatures and carriers (S/C of eight and pressure of 1 bar).

Figure 18 shows the variation of mineral constituents during the process of catalyst-enhanced steam reforming of bio-oil to recover waste heat from granulated BF slag. From Figure 18, the $CaCO_3$, CaO and complex of *2CaO*$SiO_2$ are the main mineral constituents during the process of catalyst-enhanced steam reforming of bio-oil to recover waste heat from granulated BF slag. Additionally, the $CaCO_3$ decreases but the CaO and complex of *2CaO*$SiO_2$ increase with the increasing temperature. The exothermal reaction of mineral oxide with the generated gases (Equation (13)) is the main factor affecting the $CaCO_3$, CaO and *2CaO*$SiO_2$. The exothermal reaction of mineral oxide with the generated gases (Equation (13)) shifts to the left side with the increasing temperature, decreasing the $CaCO_3$ and increasing the CaO. The increasing CaO is beneficial for obtaining the more complex *2CaO*$SiO_2$.

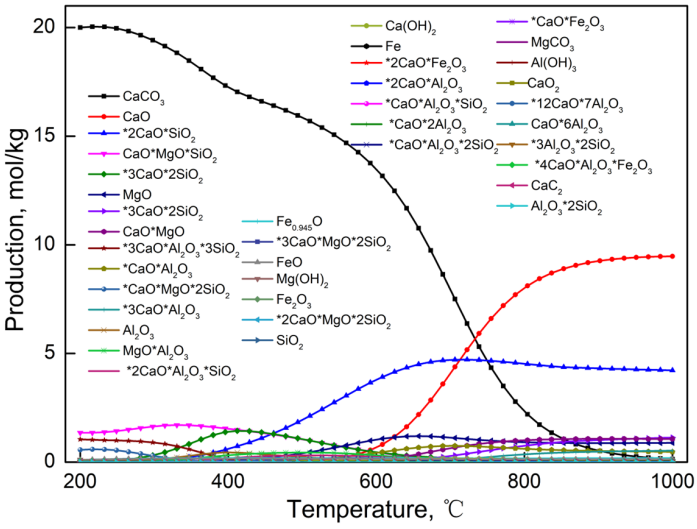


**Figure 18.** The variation of mineral constituents during the process of recovery waste heat from granulated BF slag (S/C of eight; pressure of 1 bar).

Combining the steam reforming of bio-oil [30–32] and this equilibrium calculation, the mechanism of catalyst-enhanced steam reforming of bio-oil to recover waste heat from granulated BF slag is obtained. The $Ca^{2+}$ ions in the catalyst and slag and $Fe^{3+}$ ions in the slag could improve the process of catalyst-enhanced steam reforming of bio-oil [20,32,52]. These ions could catalyze the reactants to obtain intermediate products (CxHyOz(ads), $H_2$(ads) and CxHz(ads)) [32,53], accelerating the process of catalyst-enhanced steam reforming of bio-oil to recover waste heat from granulated BF slag. The detailed mechanism of catalyst-enhanced steam reforming of bio-oil to recover waste heat from granulated BF slag is displaced in Figure 19.

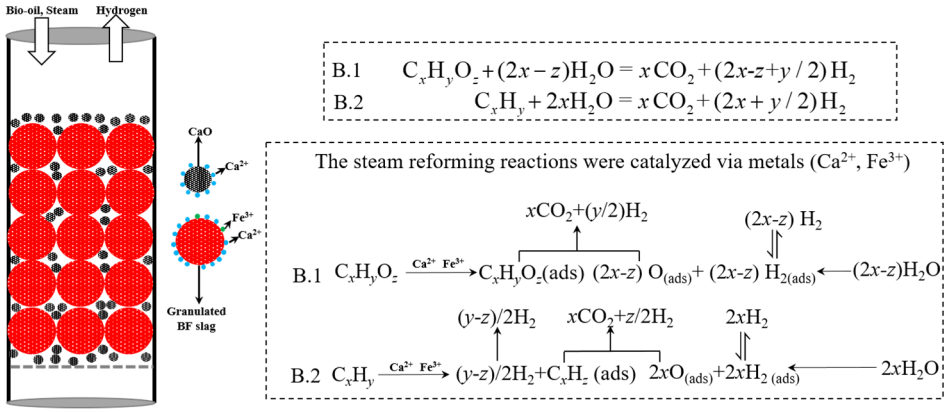


**Figure 19.** The mechanism of catalyst-enhanced steam reforming of bio-oil to recover waste heat from granulated BF slag.

## 4. Conclusions

To recover waste heat from granulated BF slag with high hydrogen yield and hydrogen component, the catalyst-enhanced steam reforming of bio-oil to recover waste heat from granulated BF slag is proposed. The equilibrium production of bio-oil enhanced steam reforming in granulated BF slag is obtained via thermodynamic calculations. The hydrogen yield, hydrogen concentration and carbon production are used for evaluating the process of catalyst-enhanced steam reforming of bio-oil in slag. Combining the practical application, the temperature of 608 °C, S/C of eight and pressure of 1 bar are regarded as the optimal conditions. At the optimal conditions, the hydrogen yield, hydrogen concentration and carbon production are 95.25%, 76.89% and 0.28 mol/kg, respectively. The catalyst could promote the hydrogen yield and hydrogen concentration. The $Ca^{2+}$ ions in the catalyst and slag and $Fe^{3+}$ ions in the slag could catalyze the reactants to obtain intermediate products, accelerating the process of catalyst-enhanced steam reforming of bio-oil to recover waste heat from slag.

**Author Contributions:** Methodology, Y.L., Z.L. and J.W.; Formal analysis, S.W.; Writing—original draft, Z.D.; Writing—review & editing, Z.D., X.Y., Y.X. and C.L. All authors have read and agreed to the published version of the manuscript.

**Funding:** This research was funded by the National Natural Science Foundation of China (52274334), the Natural Science Foundation of Hebei (E2021209106), the Youth Scholars Promotion Plan of North China University of Science and Technology (QNTJ202205), the Talent Foundation of Tangshan (A202110039), the Science and Technology Planning Project of Tangshan (22130233H), and the Funds of Basic Scientific Research of Hebei (JQN202007). And the APC was funded by the Natural Science Foundation of Hebei (E2021209106).

**Data Availability Statement:** No new data were created or analyzed in this study. Data sharing is not applicable to this article.

**Conflicts of Interest:** The authors declare no conflict of interest.

## References


1. Fan, Y.; Lu, D.; Wang, J.; Kawamoto, H. Thermochemical behaviors, kinetics and bio-oils investigation during co-pyrolysis of biomass components and polyethylene based on simplex-lattice mixture design. *Energy* **2022**, *239*, 122234.
2. Cao, Y.; Dhahad, H.A.; Hussen, H.M.; Anqi, A.E.; Farouk, N.; Issakhov, A. Development and tri-objective optimization of a novel biomass to power and hydrogen plant: A comparison of fueling with biomass gasification or biomass digestion. *Energy* **2022**, *238*, 122010.
3. Sun, Y.; Seetharaman, S.; Zhang, Z. Integrating biomass pyrolysis with waste heat recovery from hot slags via extending the C-loops: Product yields and roles of slags. *Energy* **2018**, *149*, 792–803.
4. Luo, S.; Guo, J.; Feng, Y. Hydrogen-rich gas production from pyrolysis of wet sludge in situ steam agent. *Int. J. Hydrogen Energy* **2017**, *42*, 18309–18314. [CrossRef]
5. Luo, S.; Feng, Y. The production of hydrogen-rich gas by wet sludge pyrolysis using waste heat from blast-furnace slag. *Energy* **2016**, *113*, 845–851.
6. National bureau of statistics of the People's Republic of China. China Statistical Yearbook. 2011. Available online: http://www.stats.gov.cn/tjsj/ndsj/ (accessed on 31 July 2021).
7. Yao, X.; Yu, Q.; Wang, K.; Xie, H.; Qin, Q. Kinetic characterizations of biomass char $CO_2$-gasification reaction within granulated blast furnace slag. *Int. J. Hydrogen Energy* **2017**, *42*, 20520–20528. [CrossRef]
8. Liu, J.; Yu, Q.; Zuo, Z.; Duan, W.; Han, Z.; Qin, Q.; Yang, F. Experimental investigation on molten slag granulation for waste heat recovery from various metallurgical slags. *Appl. Therm. Eng.* **2016**, *103*, 1112–1118. [CrossRef]
9. Liu, J.; Yu, Q.; Zuo, Z.; Yang, F.; Duan, W.; Qin, Q. Blast furnace slag obtained from dry granulation method as a component in slag cement. *Constr. Build. Mater.* **2017**, *131*, 381–387. [CrossRef]
10. Dhirhi, R.; Prasad, K.; Shukla, A.K.; Sarkar, S.; Renganathan, T.; Pushpavanam, S.; Kaza, M. Experimental study of rotating dry slag granulation unit: Operating regimes, particle size analysis and scale up. *Appl. Therm. Eng.* **2016**, *107*, 898–906.
11. Sun, Y.; Shen, H.; Wang, H.; Wang, X.; Zhang, Z. Experimental investigation and modeling of cooling processes of high temperatures slags. *Energy* **2014**, *76*, 761–767. [CrossRef]
12. Sun, Y.; Zhang, Z.; Liu, L.; Wang, X. Multi-Stage Control of Waste Heat Recovery from High temperatures Slags Based on Time Temperature Transformation Curves. *Energies* **2014**, *7*, 1673–1684. [CrossRef]
13. Sun, Y.; Zhang, Z.; Liu, L.; Wang, X. Heat Recovery from High temperatures Slags. A Review of Chemical Methods. *Energy* **2015**, *8*, 1917–1935.
14. Li, P. Thermodynamic analysis of waste heat recovery of molten blast furnace slag. *Int. J. Hydrogen Energy* **2017**, *42*, 9688–9695. [CrossRef]
15. Purwanto, H.; Akiyama, T. Hydrogen production from biogas using hot slag. *Int. J. Hydrogen Energy* **2006**, *31*, 491–495. [CrossRef]
16. Zhao, L.; Wang, H.; Qing, S.; Liu, H. Characteristics of gaseous product from municipal solid waste gasification with hot blast furnace slag. *J. Nat. Gas Chem.* **2010**, *19*, 403–408. [CrossRef]
17. Li, P.; Yu, Q.; Qin, Q.; Liu, J. Adaptability of coal gasification in molten blast furnace slag on coal samples and granularities. *Energy Fuels* **2011**, *25*, 5678–5682. [CrossRef]
18. Li, P.; Yu, Q.; Xie, H.; Qin, Q.; Wang, K. $CO_2$ gasification rate analysis of Datong coal using slag granules as heat carrier for heat recovery from blast furnace slag by using a chemical reaction. *Energy Fuels* **2013**, *27*, 4810–4817. [CrossRef]
19. Luo, S.; Zhou, Y.; Yi, C. Hydrogen-rich gas production from biomass catalytic gasification using hot blast furnace slag as heat carrier and catalyst in moving-bed reactor. *Int. J. Hydrogen Energy* **2012**, *37*, 15081–15085. [CrossRef]
20. Yao, X.; Yu, Q.; Xie, H.; Duan, W.; Han, Z.; Liu, S.; Qin, Q. Syngas production through biomass/$CO_2$ gasification using granulated blast furnace slag as heat carrier. *J. Renew. Sustain. Energy* **2017**, *9*, 053101. [CrossRef]
21. Sun, Y.; Zhang, Z.; Seetharaman, S.; Liu, L.; Wang, X. Characteristics of low temperatures biomass gasification and syngas release behavior using hot slag. *RSC Adv.* **2014**, *4*, 62105–62114. [CrossRef]
22. Luo, S.; Fu, J.; Zhou, Y.; Yi, C. The production of hydrogen-rich gas by catalytic pyrolysis of biomass using waste heat from blast-furnace slag. *Renew. Energy* **2017**, *101*, 1030–1036.
23. Yao, X.; Yu, Q.; Han, Z.; Xie, H.; Duan, W.; Qin, Q. Kinetic and experimental characterizations of biomass pyrolysis in granulated blast furnace slag. *Int. J. Hydrogen Energy* **2018**, *43*, 9246–9253.
24. Sun, Y.; Zhang, Z.; Liu, L.; Wang, X. Integrated carbon dioxide/sludge gasification using waste heat from hot slags: Syngas production and sulfur dioxide fixation. *Bioresour. Technol.* **2015**, *181*, 174–182. [PubMed]
25. Sun, Y.; Zhang, Z.; Liu, L.; Wang, X. Two-stage high temperatures sludge gasification using the waste heat from hot blast furnace slags. *Bioresour. Technol.* **2015**, *198*, 364–371.
26. Ma, Y.; Wang, X.R.; Li, T.; Zhang, J.; Gao, J.; Sun, Z.Y. Hydrogen and ethanol: Production, storage, and transportation. *Int. J. Hydrogen Energy* **2021**, *46*, 27330–27348.
27. Tong, L.; Yuan, Y.; Yang, T.; Bénard, P.; Yuan, C.; Xiao, J. Hydrogen release from a metal hydride tank with phase change material jacket and coiled-tube heat exchanger. *Int. J. Hydrogen Energy* **2021**, *46*, 32135–32148.
28. Setiabudi, H.D.; Aziz, M.A.A.; Abdullah, S.; The, L.P.; Jusoh, R. Hydrogen production from catalytic steam reforming of biomass pyrolysis oil or bio-oil derivatives: A review. *Int. J. Hydrogen Energy* **2020**, *45*, 18376–18397.
29. Situmorang, Y.A.; Zhao, Z.; An, P.; Yu, T.; Rizkiana, J.; Abudula, A.; Guan, G. A novel system of biomass-based hydrogen production by combining steam bio-oil reforming and chemical looping process. *Appl. Energy* **2020**, *268*, 115122.

30. Yao, X.; Yu, Q.; Xie, H.; Duan, W.; Han, Z.; Liu, S.; Qin, Q. The production of hydrogen through steam reforming of bio-oil model compounds recovering waste heat from blast furnace slag. *J. Therm. Anal. Calorim.* **2018**, *131*, 2951–2962.
31. Yao, X.; Yu, Q.; Xu, G.; Han, Z.; Xie, H.; Duan, W.; Qin, Q. The characteristics of syngas production from bio-oil dry reforming utilizing the waste heat of granulated blast furnace slag. *Int. J. Hydrogen Energy* **2018**, *43*, 22108–22115.
32. Yao, X.; Yu, Q.; Xu, G.; Han, Z.; Qin, Q. Production of syngas from dry reforming of bio-oil model compound in granulated blast furnace slag. *Korean J. Chem. Eng.* **2019**, *36*, 722–728. [CrossRef]
33. Sun, Y.; Zhang, Z.; Liu, L.; Wang, X. Integration of biomass/steam gasification with heat recovery from hot slags: Thermodynamic characteristics. *Int. J. Hydrogen Energy* **2016**, *41*, 5916–5926.
34. Feng, P.; Huang, K.; Xu, Q.; Qi, W.; Xin, S.; Wei, T.; Liao, L.; Yan, Y. Ni supported on the CaO modified attapulgite as catalysts for hydrogen production from glycerol steam reforming. *Int. J. Hydrogen Energy* **2020**, *45*, 8223–8233. [CrossRef]
35. Chen, M.; Liang, D.; Wang, Y.; Wang, C.; Tang, Z.; Li, C.; Hu, J.; Cheng, W.; Yang, Z.; Zhang, H. Hydrogen production by ethanol steam reforming over M-Ni/sepiolite (M = La, Mg or Ca) catalysts. *Int. J. Hydrogen Energy* **2021**, *46*, 21796–21811. [CrossRef]
36. Gao, N.; Salisu, J.; Quan, C.; Williams, P. Modified nickel-based catalysts for improved steam reforming of biomass tar: A critical review. *Renew. Sustain. Energy Rev.* **2021**, *145*, 111023.
37. Xie, H.; Yu, Q.; Zuo, Z.; Han, Z.; Yao, X.; Qin, Q. Hydrogen production via sorption-enhanced catalytic steam reforming of bio-oil. *Int. J. Hydrogen Energy* **2016**, *41*, 2345–2353. [CrossRef]
38. Xie, H.; Li, R.; Yu, Z.; Wang, Z.; Yu, Q.; Qin, Q. Combined steam/dry reforming of bio-oil for $H_2$/CO syngas production with blast furnace slag as heat carrier. *Energy* **2020**, *200*, 117481.
39. Ma, Z.; Xiao, R.; Zhang, H. Catalytic steam reforming of bio-oil model compounds for hydrogen-rich gas production using bio-char as catalyst. *Int. J. Hydrogen Energy* **2017**, *42*, 3579–3585. [CrossRef]
40. Wang, S.; Cai, Q.; Zhang, F.; Li, X.; Zhang, L.; Luo, Z. Hydrogen production via catalytic reforming of the bio-oil model compounds: Acetic acid, phenol and hydroxyacetone. *Int. J. Hydrogen Energy* **2014**, *39*, 18675–18687.
41. Xie, H.; Yu, Q.; Yao, X.; Duan, W.; Zuo, Z.; Qin, Q. Hydrogen production via steam reforming of bio-oil model compounds over supported nickel catalysts. *J. Energy Chem.* **2015**, *24*, 299–308. [CrossRef]
42. Yao, X.; Yu, Q.; Wang, K.; Xie, H.; Qin, Q. Kinetic study on recovery heat of granulated blast-furnace slag through biomass gasification using $CO_2$ as gasification agent. *J. Therm. Anal. Calorim.* **2018**, *131*, 1313–1321. [CrossRef]
43. Yao, X.; Yu, Q.; Han, Z.; Xie, H.; Duan, W.; Qin, Q. Kinetics of $CO_2$ gasification of biomass char in granulated blast furnace slag. *Int. J. Hydrogen Energy* **2018**, *43*, 12002–12012. [CrossRef]
44. Duan, W.; Yu, Q.; Xie, H.; Qin, Q.; Zuo, Z. Thermodynamic analysis of hydrogen-rich gas generation from coal/steam gasification using blast furnace slag as heat carrier. *Int. J. Hydrogen Energy* **2014**, *39*, 11611–11619. [CrossRef]
45. Duan, W.; Yu, Q.; Xie, H.; Liu, J.; Wang, K.; Qin, Q.; Han, Z. Thermodynamic analysis of synergistic coal gasification using blast furnace slag as heat carrier. *Int. J. Hydrogen nergy* **2016**, *41*, 1502–1512. [CrossRef]
46. Xie, H.; Yu, Q.; Zhang, Y.; Zhang, J.; Liu, J.; Qin, Q. New process for hydrogen production from raw coke oven gas via sorption-enhanced steam reforming: Thermodynamic analysis. *Int. J. Hydrogen Energy* **2017**, *42*, 2914–2923.
47. Xie, H.; Yu, Q.; Lu, H.; Zhang, Y.; Zhang, J.; Qin, Q. Thermodynamic study for hydrogen production from bio-oil via sorption-enhanced steam reforming: Comparison with conventional steam reforming. *Int. J. Hydrogen Energy* **2017**, *42*, 28718–28731.
48. Xie, H.; Yu, Q.; Zuo, Z.; Zhang, J.; Han, Z.; Qin, Q. Thermodynamic analysis of hydrogen production from raw coke oven gas via steam reforming. *J. Therm. Anal. Calorim.* **2016**, *126*, 1621–1631. [CrossRef]
49. Xie, H.; Yu, Q.; Wei, M.; Duan, W.; Yao, X.; Qin, Q.; Zuo, Z. Hydrogen production from steam reforming of simulated bio-oil over Ce–Ni/Co catalyst with in continuous $CO_2$ capture. *Int. J. Hydrogen Energy* **2015**, *40*, 1420–1428. [CrossRef]
50. Xie, H.; Zhang, J.; Yu, Q.; Zuo, Z.; Liu, J.; Qin, Q. Study on Steam Reforming of Tar in Hot Coke Oven Gas for Hydrogen Production. *Energy Fuels* **2016**, *30*, 2336–2344. [CrossRef]
51. Xie, H.; Yu, Q.; Wang, K.; Shi, X.; Li, X. Thermodynamic analysis of hydrogen production from model compounds of bio-oil through steam reforming. *Environ. Prog. Sustain. Energy* **2014**, *33*, 1008–1016.
52. Luo, S.; Feng, Y. The production of fuel oil and combustible gas by catalytic pyrolysis of waste tire using waste heat of blast-furnace slag. *Energy Convers. Manag.* **2017**, *136*, 27–35. [CrossRef]
53. Duan, W.; Yu, Q.; Liu, J.; Wu, T.; Yang, F.; Qin, Q. Experimental and kinetic study of steam gasification of low-rank coal in molten blast furnace slag. *Energy* **2016**, *111*, 859–868. [CrossRef]